Proceedings of The Institute of Acoustics

THE DESIGN AND IMPLEMENTATION OF A DIGITAL INTEGRATOR FOR USE IN AN ACTIVE VIBRATION CONTROL SYSTEM

T. Hodges, P.A. Nelson and S.J. Elliott

Institute of Sound and Vibration Research, The University of Southampton, Southampton SO9 5NH, England.

1. INTRODUCTION

Many situations arise in which the control of vibration is necessary; for example, reciprocating machinery may transmit large periodic forces which result in excessive vibration levels at another point. In space structures, vibration may cause problems where high accuracy is required in devices such as space telescopes or satellite transmission systems. Two broad categories of vibration control systems exist; passive systems which contain energy storing and dissipative components, and active systems which use secondary sources of energy to attempt to reduce the overall system energy in some pre-determined way. In many situations, use of passive methods of isolation will give adequate results. Active control, however, may be used to good effect in situations where passive systems are less efficient, such as at low frequencies, or where use of passive methods would lead to the addition of too much mass to a system. In addition, an active system can be made "adaptive" so that parameter variations may be tracked, and for deterministic inputs in particular, the system may actually "preview" the disturbance and then attempt to control it in some way.

The active control of vibration has been considered in many areas. These have ranged from its use to control transverse vibrations of circular saw blades [1] to active vibration isolation of parts of a helicopter fuselage [2]. Its use has also been considered in the control of tall buildings [3] and has been proposed for the control of lightly-damped space structures [4,5]. In most cases, the overall control strategy is similar, consisting of the feedback of some measured variables in such a way as to either alter the modal characteristics of the structure [6] or to synthesise an opposing force in an attempt to cancel out the vibration completely.

The work presented in this paper shows the alteration of the modal parameters (damping ratio and natural frequency) of the fundamental mode of transverse vibration of a cantilever beam, using feedback control techniques. The equation of motion is solved for the beam, yielding the usual series of natural frequencies and mode shapes. In order to use feedback control on a simplified model, this multi-modal system is then considered as a single fundamental mode plus a residual contribution from the higher order modes. Use of series expansions allows an evaluation of the residual term, which is shown to be small by comparison with the response of the beam at its fundamental frequency. By making this assumption, and also by careful design of the experimental apparatus, the modelling of a cantilever beam as a single degree of freedom system is justified. Using this model, the theoretical alteration of natural frequency and damping ratio may be simply illustrated, from which the design of a proportional-plus-integral-plus-derivative (PID) controller to perform this task is proposed. It is shown that in order to perform this experimentally using a digital control system, accurate integration must be performed digitally.

The design of such integrators is shown to be more complex than is suggested by previous theoretical work, and the final version is designed in order to account for time delays within the digital system due to sample-hold devices on the output stages of the system. Other design approaches are described and the results obtained (in terms of frequency response magnitude, phase and stability) are given. The PID controller is used to alter the natural frequency and damping of the fundamental mode of vibration of the cantilever beam system described earlier.

2. THEORY

2.1 Equation of Motion

The equation of motion of a uniform beam in transverse motion [7], subject to an applied force $f(x,t)$ is:

$$EI \frac{\partial^4 y}{\partial x^4} + m \frac{\partial^2 y}{\partial t^2} = f(x,t) \qquad (1)$$

where y represents the transverse displacement (m), x represents the distance along the beam (m), E is the Young's modulus of the beam (N/m^2), I is the second moment of area of the beam (m^4) and m is the mass per unit length of the beam (kg/m).

This equation may be shown to have a solution of the form

$$y(x,t) = \sum_{n=1}^{\infty} q_n(t)\phi_n(x) \qquad (2)$$

where $q_n(t)$ represents a generalised coordinate, and $\phi_n(x)$ the mode shape function. It is seen that the theoretical solution considers the beam response to consist of an infinite number of modes of vibration. Obviously, for the purposes of any practical system model, the number of modes considered must be reduced. The modal series expansion of equation (2) may be written in the form

$$y(x_1,x_2,\omega) = \sum_{n=1}^{N} \frac{(\phi_n(x_1)\phi_n(x_2))Q}{\omega_n^2[1 - (\omega/\omega_n)^2 + j2\zeta_n]} \qquad (3)$$

where $\phi_n(x_i)$ is the mass-normalised mode shape function for the n'th mode at point i, ω_n and ζ_n are the natural frequency and damping ratio of the n'th mode respectively, and the $e^{j\omega t}$ time dependence of the forcing term Q has been suppressed. A viscous damping model has been used in preference to the hysteretic damping model because, although use of hysteretic damping may allow for more accurate representation of physical material properties, its use introduces a non-causal impulse response and assumes that a sinusoidal disturbing force is used [7].

2.2 Single Degree of Freedom System Model

The transfer mobility function between points 1 and 2 $M_{12}(j\omega)$ may be written

$$M_{12}(j\omega) = \dot{y}(x_1, x_2, \omega)/(Q)$$

$$= \sum_{n=1}^{N} \frac{j\omega A_{12}^{(n)}}{\omega_n^2[1 - (\omega/\omega_n)^2 + j2\zeta_n]} \qquad (4)$$

where $A_{12}^{(n)} = \Phi_n(x_1)\Phi_n(x_2)$.

For a continuous structure, $N \rightarrow \infty$ and so in practice the function $M_{12}(j\omega)$ must be approximated by

$$M_{12}[\infty] = M_{12}[n_1] + R \qquad (5)$$

i.e., the contribution of n_1 modes plus an error, or "residual" term. In order to model the structure simply, the magnitude of the residual term relative to that due to the modelled modes must be assessed. As stated earlier, ideally one would like to only require a model which has one mode. The residual term R may be written

$$R = \sum_{n=n_1+1}^{\infty} \frac{j\omega A_{12}^{(n)}}{\omega_n^2[1 + (\omega/\omega_n)^2 + j2\zeta_n} \qquad (6)$$

Assuming that the excitation frequency is well below the resonant frequency of the higher modes (i.e., $[\omega/\omega_n]^2 << 1$) and that $2\zeta_n << 1$ then

$$R = j\omega \sum_{n=n_1+1}^{\infty} \frac{A_{12}^{(n)}}{\omega_n^2} \qquad (7)$$

For a cantilever beam [7] one may make the approximation

$$\omega_n \approx \omega_o[2n - 1]^2$$

which leads to the expression

$$R = \frac{j\omega}{\omega_o^2} \sum_{n=n_1+1}^{\infty} \frac{A_{12}^{(n)}}{(2n - 1)^4} \qquad (8)$$

Then, taking as a worst case, $A_{12}^{(n)} = 1;\ n = n_1, \ldots, \infty$ this yields

$$R = \frac{-j\omega}{\omega_o^2} \sum_{n=n_1+1}^{\infty} \frac{1}{(2n-1)^4}$$

which is a series of the form

$$\left[\sum_{n=1}^{\infty} \frac{1}{(2n-1)^4} - \sum_{n=1}^{n_1} \frac{1}{(2n-1)^4}\right]$$

and using the result [8] that

$$\sum_{n=1}^{\infty} \frac{1}{(2n-1)^4} = \pi^4/96$$

therefore may be written as

$$R = \frac{-j\omega}{\omega_o^2} \left[\frac{\pi^4}{96} - \sum_{n=1}^{n_1} \frac{1}{(2n-1)^4}\right] \qquad (9)$$

Note that this may be easily evaluated, since n_1 is small.

In order to accurately model a cantilever beam as a single mode system, then a high value of ω_o should be used so that the modal separation is high and hence the residual term at the fundamental frequency is low.

If this is true, then the beam may be modelled as a standard second-order system with mass m, damping c and spring stiffness k. The equation of motion of the beam in response to a force $f(t)$ then becomes

$$m\ddot{x}(t) + c\dot{x}(t) + kx(t) = f(t) \qquad (10)$$

where m, c and k represent modal masses, damping and stiffness terms respectively.

In order to apply active control to the system, assume that signals corresponding to the acceleration, velocity and displacement of the beam may be obtained, and fed back, scaled by gains M_C, C_C and K_C respectively, as shown in Figure 1. The equation of motion must be modified in order to account for the feedback terms and becomes

$$m\ddot{x} + c\dot{x} + kx = f + u$$

where $u = -(M_C\ddot{x} + C_C\dot{x} + K_Cx)$ is the force signal fed back into the structure, i.e.,

$$(m + M_C)\ddot{x} + (c + C_C)\dot{x} + (k + K_C)x = f(t) \qquad (11)$$

Thus, modification of the natural frequency and/or damping ratio of the beam is now possible by appropriate choice of gains M_C, C_C and K_C. This will result in a modified fundamental frequency ω_o' and damping ratio ζ_o' given by:

$$\omega_o' = \left[\frac{k + K_C}{m + M_C}\right]^{1/2}$$

and

$$\zeta_o' = \frac{(c + C_C)}{2\sqrt{(k + K_C)(m + M_C)}}$$

By alteration of the gains M_C or K_C then the fundamental frequency of the structure may be either increased ($K_C > 0$ or $M_C < 0$) or decreased ($M_C > 0$ or $K_C < 0$). These changes correspond to changes in the *apparent mass* and *apparent stiffness* respectively of the beam. It is important to note that no *physical* addition of stiffness or mass has taken place. In a similar way, use of velocity feedback ($C_C \neq 0$) allows alteration of the modal damping of the structure.

By inspection of the roots of equation (11) for all values of the coefficients, it is seen that stability of the system is in principle assured provided that $(m + M_C)$, $(c + C_C)$ and $(k + K_C) > 0$.

2.3 Design of a PID Controller

In order to feed signals corresponding to acceleration, velocity and displacement back into a structure, the classical PID controller [9] is of the form shown in Figure 2. In this case the output $y(t)$ is related to the input $u(t)$ by

$$y(t) = K_P\, u(t) + K_I \int u(t)dt + K_D \frac{\partial u(t)}{\partial t} \qquad (12)$$

THE DESIGN AND IMPLEMENTATION OF A DIGITAL INTEGRATOR FOR USE IN AN ACTIVE VIBRATION CONTROL SYSTEM

In most practical cases, the surface acceleration of a structure is the input signal $u(t)$. The controller must therefore be reformulated as in Figure 3. It is now seen that accurate digital integration is required in order to achieve the objective of obtaining and feeding back acceleration, velocity and displacement signals. The following section describes the design and implementation of the integrators required for such a task.

2.4 Design of a Precision Digital Integrator

Two approaches to the design of a digital integrator are possible; either design the device directly in the digital domain, or map (using some specified transformation) on analogue design into the digital domain [10].

A problem unique to digital systems is immediately encountered when designing such a device. Two features inherent to the system cause delays, and hence inaccuracies in the phase response (which, for perfect integration, should have a value of $-\pi/2$ for all values of ωT in the range $0 \leq \omega T \leq 2/T$, where T is the sample period). These are:

(i) the sample-hold devices on the output of the digital system, which have a $(\sin \omega T/\omega T)$ type transfer function and hence give rise to a ½-sample delay [10], and

(ii) the finite processing time of the processor used to implement the algorithm, which will add a further delay. This may be reduced (for a given processor) by reducing the code implemented per sample to a minimum.

Two design approaches will be shown here, both involving transformation of an analogue design into the digital z-plane.

2.4.1 Bilinear transform design [10]

The analogue model used has a transfer function of the form $H(s) = a/(s + a)$ where a is a constant. Making the substitution

$$s = \left(\frac{2}{T}\right)\left(\frac{z - 1}{z + 1}\right)$$

where T is the sample period, which corresponds to the bilinear transform, then

$$H(z) = \frac{a(1 + z^{-1})}{(a + 2/T) + (a - 2/T)z^{-1}} \qquad (13)$$

Evaluation of the frequency response of this design by setting $z = e^{j\omega T}$ with $T = 0.001$ (i.e., a sampling frequency of 1 kHz) and $a = 1$ yields the response of Figure 4. Two features are apparent:

(i) the design gives a unit gain at d.c., and

(ii) although no account has been taken of any phase terms introduced by the features described earlier in section 2.4, the response tends towards a value of $-\pi/2$. When these terms are added to the phase response, it will not be a good approximation to an integrator.

2.4.2 Impulse invariant transform design [10]

The analogue integrator transfer function used is again

$$H(s) = a/s + a$$

inverse Laplace transforming this gives

$$h(t) = ae^{-at}$$

so that an impulse invariant transformation yields

$$h(nT) = ae^{-anT}$$

where T is the sample period.

This response may now be transformed into the z-plane, giving

$$H(z) = \frac{a}{1 - e^{-aT}z^{-1}} \qquad (14)$$

Setting $z = e^{j\omega T}$ and evaluating $H(e^{j\omega T})$ for $0 \leq \omega T \leq \pi/2$ yields the frequency response of Figure 5 (again $a = 1$ and $T = 0.001$). Examination of Figure 5 shows that:

(i) the magnitude response has a large value at d.c., and

(ii) the phase response reaches a value of $-\pi/2$ very quickly but then slopes uniformly up to 0 at $\omega T = \pi$ (i.e., at a frequency of half the sample rate; 500 Hz in this example).

The phase response is of the form

$$\mathrm{Arg}[H(e^{j\omega T})] = \tan^{-1}\left[\frac{-e^{-aT}\sin\omega T}{1 - e^{-aT}\cos\omega T}\right] \qquad (15)$$

For $e^{-aT} \simeq 1$, i.e., $(aT \to 0)$, then equation (15) becomes

$$\mathrm{Arg}[H(e^{j\omega T})] \simeq \tan^{-1}\left[\frac{-\sin\omega T}{1 - \cos\omega T}\right]$$

The use of the approximation ($aT \to 0$) may be justified since for most practical systems, T is as small as possible, and, since integration is required from low frequencies, a is also set to a small value. For the example here, $aT = 0.001$ and therefore the error in assuming that $e^{-aT} = 1$ is of the order of 0.1%.

Equation (15) may be further rewritten as

$$\mathrm{Arg}[H(e^{j\omega T})] \simeq \tan^{-1}\left[\frac{2\sin(\omega T/2)\cos(\omega T/2)}{2\cos^2(\omega T/2)}\right]$$

$$\simeq \tan^{-1}(\cot \omega T/2)$$

By use of addition formulae, this may be expressed as

$$\mathrm{Arg}[H(e^{j\omega T})] = (\omega T/2) - (\pi/2) \qquad (16)$$

i.e., when the half-sample delay due to the sample-hold circuits is included, the phase response will be almost exactly $-\pi/2$ for $0 \leq \omega T \leq \pi$, as required. The extra delay due to the finite speed of the processor will still be incurred, but in general this may be made of much smaller magnitude. Hence the implementation of equation (14) in difference equation form will give accurate digital integration with the sample-hold delays already accounted for. This form of integrator was used to perform the experimental work described in section 3 of this paper.

3. EXPERIMENTAL PROCEDURE

The apparatus used to perform the work is shown in Figure 6. The cantilever beam used has a fundamental frequency of approximately 90 Hz. This ensures that the modal separation is high, and thus in equation (9) the residual term is approximately $j\omega.5 \times 10^{-8}$ which is of much lower magnitude than the response of the fundamental mode at resonance which is of the order of 0.2. In addition, the excitation force was a bandlimited random signal with an upper frequency limit of 250 Hz, in order to excite only the fundamental mode. The impedance head was mounted at a position corresponding to a node of the second cantilever resonance. In this way the approximation of the beam to a second order system was achieved.

In all the experimental work, a Texas Instruments TMS 32020 Digital Signal Processor operating at a sample rate of 44 kHz was used to provide digital integration. The processor operates at 5 MHz, giving an instruction cycle time of 200 msec.

4. RESULTS AND DISCUSSION

Figure 7 shows the modulus of inertance of the beam up to 1.6 kHz with no active control applied. Figure 8 shows the modulus of inertance with active control applied in the form of velocity feedback (i.e., $C_C \neq 0$, $M_C = K_C = 0$). Attenuation of 19.5 dB is achieved at the fundamental frequency, with attenuation of ≃ 6 dB at the second mode. The reduced attenuation is due to the decrease of damping ratio with frequency, which requires that higher gains be used at higher frequencies. By contrast, the gain in the feedback path decreases monotonically with frequency due to the contribution of the integrator.

Figure 9 shows the result of performing displacement and velocity feedback (i.e., in this case integral and double-integral control, so that $M_C = 0$, C_C and $K_C \neq 0$). The resonant frequency has been shifted from 90 Hz to 137 Hz, and the added damping has reduced the amplitude of the mode by some 6 dB. This shift in natural frequency corresponds to an increase in stiffness by a factor 2.3. Figure 10 shows an example of proportional and integral control, corresponding to acceleration-plus-velocity feedback. The fundamental has been shifted in frequency from 90 Hz to 81.5 Hz and its amplitude increased (which corresponds to $C_C < 0$) by almost 5 dB.

The results show clearly that by selection of the correct combinations of gains, the PID-type controller may be used to adjust the modal parameters of the simple system used. The primary advantage of the digital controller over its analogue counterpart is the ease with which the control parameters may be altered, and the precision with which they may be selected.

The integrator performs well, with a phase response which is accurate to within less than 1° above about 3 Hz. The delays due to the finite processor time are small; each instruction cycle takes 200 nsec to perform, so that the entire algorithm is executed within 8 μsec. The processor, even while operating at a sample rate of 44 kHz (cycle time of 24 μsec) is idle for ≃ 70% of the time. The actual delay that this represents when operating at such low frequencies (relative to the sample rate) is therefore low. This feature is still of importance, however, in two cases:

(i) when the frequency range of interest is higher, and the code to be implemented is more complex, and

(ii) when the code is of variable length (due to branches/jumps in execution). This will cause "jitter" on the output unless precautions are taken to latch the output in some way.

5. CONCLUSIONS

The alteration of modal parameters using a digital controller is illustrated. The design of the controller is based around the design of a very accurate digital integrator. This design is examined in detail, together with a discussion of features such as internal delays which pose many of the problems involved with the practical implementation of such control algorithms.

THE DESIGN AND IMPLEMENTATION OF A DIGITAL INTEGRATOR FOR USE IN AN ACTIVE VIBRATION CONTROL SYSTEM

REFERENCES

1. R.W. ELLIS and C.D. MOTE 1979 Trans. ASME, Journal of Dynamic Systems, Meas. and Control 101, 44-49. A feedback vibration controller for circular saws.

2. G. SCHULZ 1979 Automatica 15, 461-466. Active multivariable vibration isolation for a helicopter.

3. J. ROORDA 1975 ASCE J. Struc. Divn. 101, 505-521. Tendon control in tall structures.

4. M.J. BALAS 1979 J. Guidance and Control 2, 252-253. Direct velocity feedback control of large structures in space.

5. P.C. HUGHES and T.M. ABDEL-RAHMAN 1979 J. Guidance and Control 2, 499-503. Stability of proportional-plus-derivative-plus-integral control of flexible spacecraft.

6. T. HODGES, P.A. NELSON and S.J. ELLIOTT 1986 Presented at Euromech Colloquium 213 "Methodes Actives de Controle du Bruit et des Vibrations", CNRS, Marseille. The active simulation of structural frequency response.

7. W.T. THOMSON 1981 Theory of Vibration with Applications. 2nd edition. George Allen and Unwin, London.

8. M.R. SPIEGEL 1968 Mathematical Handbook of Formulas and Tables. Mc-Graw-Hill Book Co., New York.

9. R.J. RICHARDS 1979 An Introduction to Dynamics and Control. Longman.

10. B.C. KUO 1981 Digital Control Systems. Holt-Saunders International Editions, Japan.

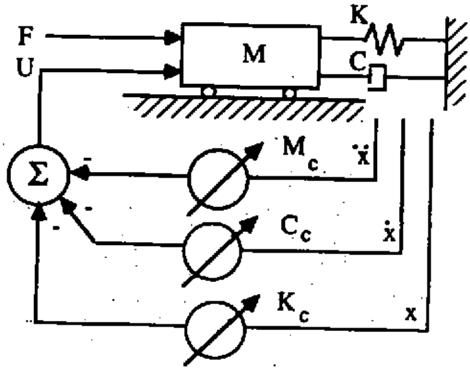

Figure 1 : Representation of system with feedback terms included.

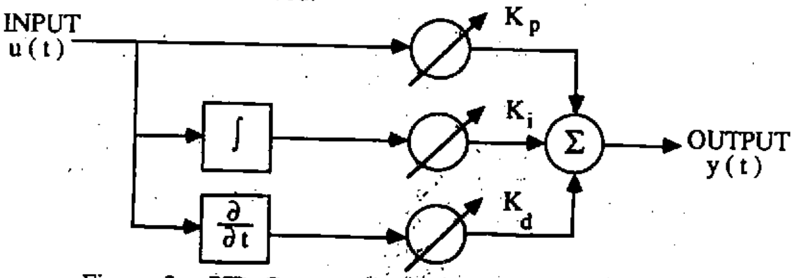

Figure 2 : PID Controller - Classical Design.

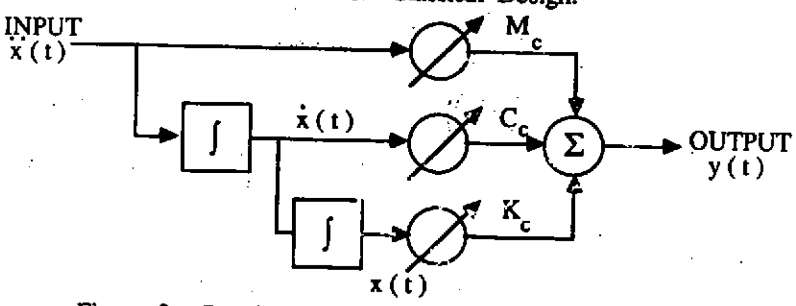

Figure 3 : Practical Implementation of a PID Controller.

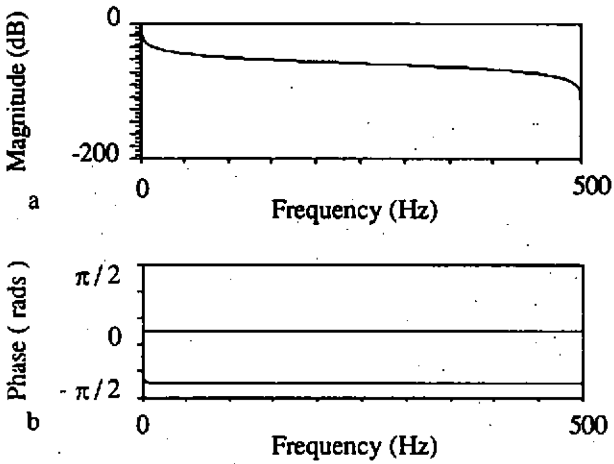

Figure 4 : Integrator frequency response - bilinear transform method
a. Magnitude
b. Phase

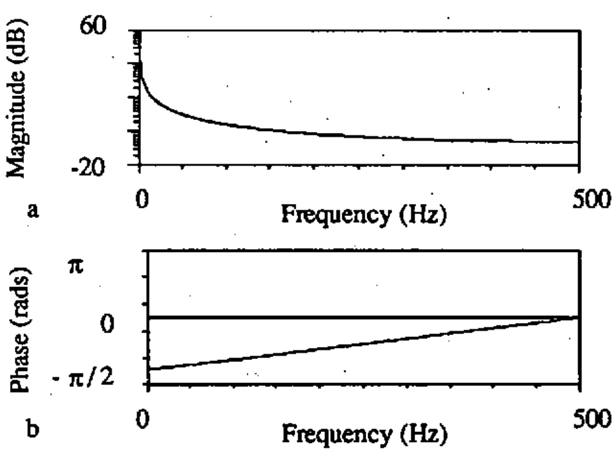

Figure 5 : Frequency response of integrator - impulse invariant design
a. Magnitude
b. Phase

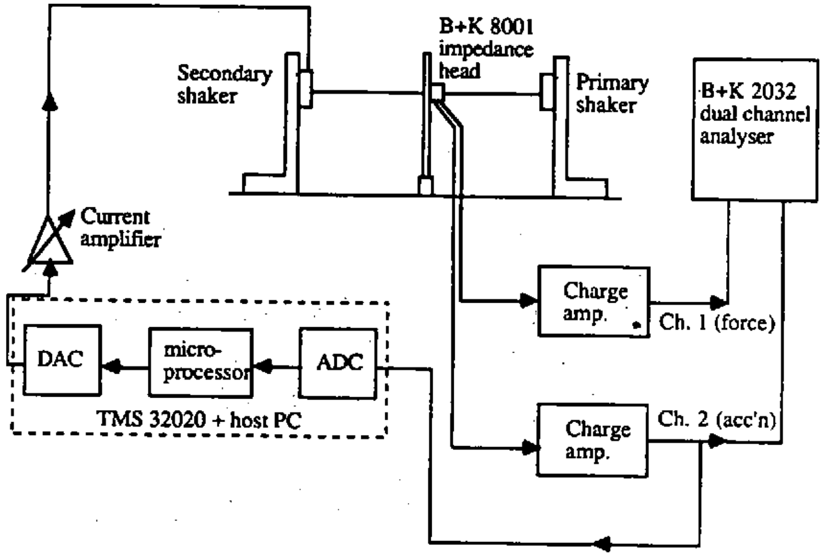

Figure 6 : Experimental apparatus

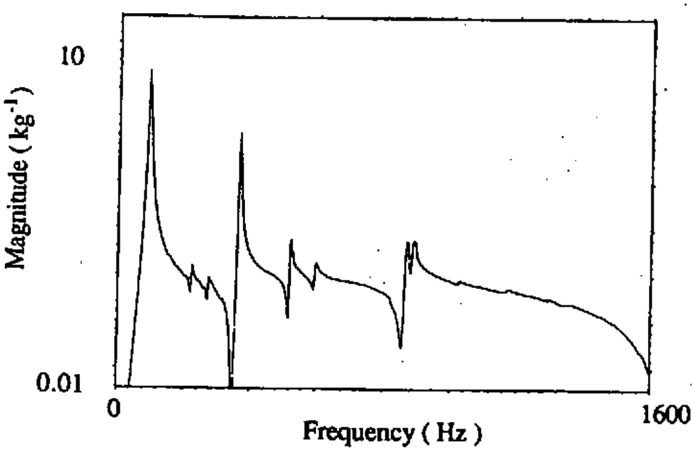

Figure 7 : Cantilever Beam Inertance - No Active Control.

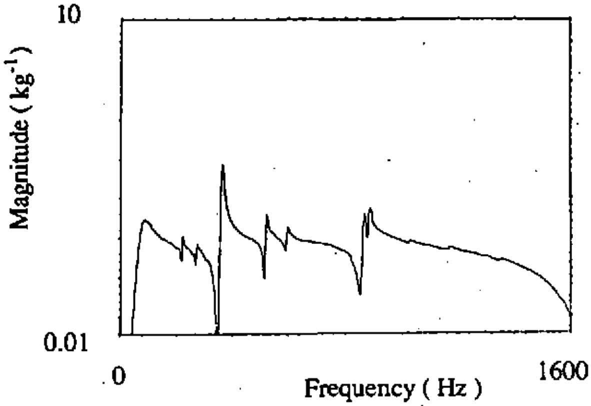

Figure 8 : Cantilever Beam Inertance - Active Control Applied.

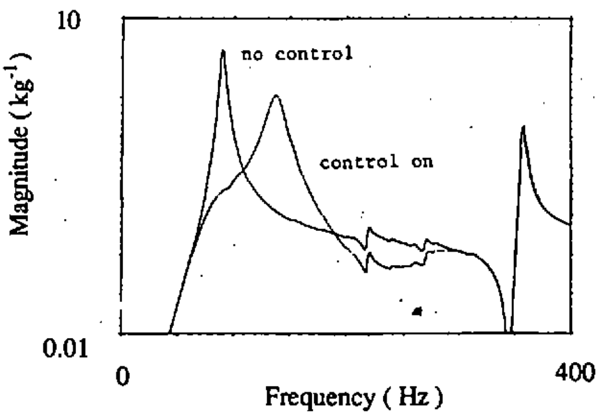

Figure 9 : Integral plus Double Integral Control
(i.e. velocity plus displacement feedback).

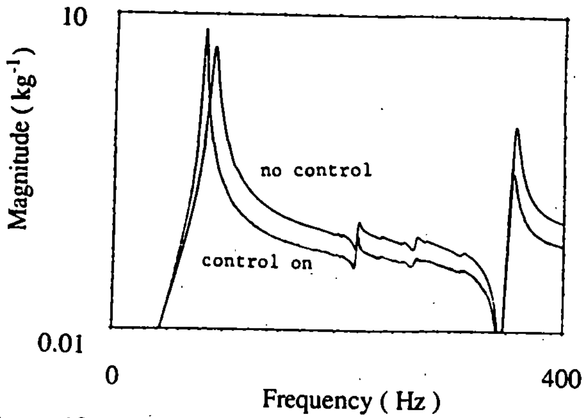

Figure 10 : Proportional plus Integral Control (i.e. acceleration plus velocity feedback).